

1 **Microglia are Required for Developmental Specification of AgRP**
2 **Innervation in the Hypothalamus of Offspring Exposed to Maternal High Fat**
3 **Diet During Lactation**

4
5
6

7 Haley N. Mendoza-Romero, Jessica E. Biddinger, Michelle N. Bedenbaugh and Richard B.
8 Simerly¹

9

10 Dept of Molecular Physiology & Biophysics, Vanderbilt University, Nashville, TN, 37232, USA

11
12

13 **¹Corresponding author:** Richard B. Simerly

14 **Email:** richard.simerly@vanderbilt.edu

15
16
17

18 **Competing Interest Statement:** No competing interests

19

20 **Classifications:** Major category: Developmental Biology; Minor category: Neuroscience

21
22
23

24 **Keywords:**

25 Microglia
26 Neural Development
27 Hypothalamus
28 Agouti-related peptide
29 Paraventricular hypothalamic nucleus

30
31

32

33 **Abstract**

34

35 Nutritional fluctuations that occur early in life dictate metabolic adaptations that will affect
36 susceptibility to weight gain and obesity later in life. The postnatal period in mice represents a
37 time of dynamic changes in hypothalamic development and maternal consumption of a high fat
38 diet during the lactation period (MHFD) changes the composition of milk and leads to
39 enhanced susceptibility to obesity in offspring. Agouti-related peptide (AgRP) neurons in the
40 arcuate nucleus of the hypothalamus (ARH) react to changes in multiple metabolic signals and
41 distribute neuroendocrine information to other brain regions, such as the paraventricular
42 hypothalamic nucleus (PVH), which is known to integrate a variety of signals that regulate
43 body weight. Development of neural projections from AgRP neurons to the PVH occurs during
44 the lactation period and these projections are reduced in MHFD offspring, but underlying
45 developmental mechanisms remain largely unknown. Microglia are the resident immune cells
46 of the central nervous system and are involved in refinement of neural connections and
47 modulation of synaptic transmission. Because high fat diet exposure causes activation of
48 microglia in adults, a similar activation may occur in offspring exposed to MHFD and play a
49 role in sculpting hypothalamic feeding circuitry. Genetically targeted axonal labeling and
50 immunohistochemistry were used to visualize AgRP axons and microglia in postnatal mice
51 derived from MHFD dams and morphological changes quantified. The results demonstrate
52 regionally localized changes to microglial morphology in the PVH of MHFD offspring that
53 suggest enhanced surveillance activity and are temporally restricted to the period when AgRP
54 neurons innervate the PVH. In addition, axon labeling experiments confirm a significant
55 decrease in AgRP innervation of the PVH in MHFD offspring and provide direct evidence of
56 synaptic pruning of AgRP inputs to the PVH. Microglial depletion with the Colony-stimulating
57 factor 1 receptor inhibitor PLX5622 determined that the decrease in AgRP innervation
58 observed in MHFD offspring is dependent on microglia, and that microglia are required for
59 weight gain that emerges as early as weaning in offspring of MHFD dams. However, these
60 changes do not appear to be dependent on the degree of microglial mediated synaptic
61 pruning. Together, these findings suggest that microglia are activated by exposure to MHFD
62 and interact directly with AgRP axons during development to permanently alter their density,
63 with implications for developmental programming of metabolic phenotype.

64

65 **Significance Statement**

66

67 Maternal high fat diet exposure results in enhanced risk for negative health outcomes in
68 humans and multiple animal models. Here we demonstrate that microglia are required for
69 changes in body weight and perturbations to hypothalamic circuits caused by maternal high fat
70 diet exposure that is limited to the lactational period. We identified spatially and temporally
71 limited morphological changes to microglia that reflect an enhancement of surveillance activity
72 and align with a critical period of hypothalamic circuit formation. We also identify direct cellular
73 interactions between microglia and developing axons, as well as evidence for synaptic
74 engulfment, although this mechanism does not appear to be responsible for changes to neural
75 patterning caused by maternal high fat diet exposure. Together these findings identify an
76 essential role for microglia in specifying patterns of hypothalamic innervation during

77 development in response to maternal high fat diet exposure, which may contribute to
78 developmental programming of metabolic phenotype.

79
80

81 **1 Introduction**

82

83 Maternal nutritional status has a profound effect on the metabolic phenotype of offspring.
84 Children born to obese mothers experience higher rates of obesity later in life, with
85 accompanying comorbidities that negatively impact health and longevity (Stettler et al., 2005;
86 Prospective Studies Collaboration et al., 2009; Tamashiro and Moran 2010; Andersen et al.,
87 2012). Although this developmental programming of metabolic phenotype has been
88 reproduced in a number of animal models (Samuelsson et al., 2008; Masuyama et al., 2014;
89 Garcia-Caceres et al., 2019; Skowronski, Leibel and Leduc, 2023), the underlying mechanisms
90 remain poorly defined. In mouse models, maternal obesity during lactation (MHFD), a time
91 when offspring are dependent on milk from their mothers for nutrition, appears to be
92 particularly impactful. These changes to metabolic phenotype are thought to be mediated by
93 changes in the milk (Gorski et al., 2006; Vogt et al., 2014; Calvo-Lerma et al., 2022) and occur
94 without subsequent dietary challenge to the offspring themselves, suggesting that they are a
95 consequence of developmental programming (Bolton et al., 2022; Skowronski, Leibel and
96 LeDuc, 2023). Because neural circuits known to control body weight develop during the
97 lactational period, they are vulnerable to a variety of environmental signals that may affect their
98 organization and function (Horvath et al., 2010; Elson and Simerly 2015; Bouret, Levin and
99 Ozanne, 2015; Zeltser, 2018; Skowronski, Leibel and Leduc, 2023).

100

101 AgRP neurons in the arcuate nucleus of the hypothalamus (ARH) function as “hunger neurons”
102 that respond to key metabolic signals such as leptin, ghrelin, glucose and free fatty acids
103 (Krashes et al., 2011; Betley et al., 2015; Chen et al., 2015; Sutton Hickey et al., 2023), and
104 they distribute this information to other regions associated with energy balance regulation
105 (Simerly 2008; Zagmutt, et al., 2018). Thus, the ability of AgRP neurons to influence other
106 components of feeding circuitry is dependent on formation of their neural connections, which
107 form primarily during the first 2 weeks of life (Bouret, Draper and Simerly, 2004a). During
108 development, AgRP axons extend from the ARH at postnatal day 4 (P4) and reach the
109 paraventricular hypothalamic nucleus (PVH) between P8-P10. Leptin is required for normal
110 targeting of AgRP axons to their downstream targets, and in leptin deficient mice both
111 neuroanatomical and related physiological defects persist into adulthood (Bouret et al., 2004b;
112 Bouyer et al., 2013; Elson and Simerly 2015). Maternal overnutrition affects formation of
113 feeding circuits during postnatal life with concomitant dysregulation of body weight (Plagemann
114 et al., 1992; Elson and Simerly, 2015; Lippert and Bruning, 2022; Skowronski, Leibel and
115 LeDuc, 2023). Limiting high fat diet exposure of dams to the first 3 weeks of lactation (MHFD)
116 causes suppression of neural projections from AgRP neurons to the PVH in offspring and is
117 associated with increased body weight later in life (Vogt et al., 2014). In fact, MHFD was more
118 effective than prenatal maternal high fat diet exposure in causing body weight changes of adult
119 offspring. MHFD did not alter cell number, peptidergic expression, or cellular activity of AgRP
120 neurons in the ARH, suggesting that maternal nutritional status during lactation is particularly
121 important for the establishment of neural connections related to the control of body weight.

122 Notably, the effects of both leptin (Kamitakahara et al., 2018) and MHFD (Vogt et al., 2014) on
123 targeting of AgRP projections display considerable regional specificity.

124
125 Adult mice placed on HFD display a marked hypothalamic gliosis that reveals an acute
126 inflammatory response, which presages significant weight gain (Horvath et al., 2010;
127 Valdearcos et al., 2017; Spencer et al., 2019; Cansell et al., 2021). This hypothalamic
128 neuroinflammation is characterized by marked changes in the density and morphology of
129 microglia that are most pronounced in the ARH (Thaler et al., 2012; Valdearcos et al., 2014).
130 Microglia are the resident myeloid cells of the CNS and respond to a broad array of circulating
131 signals, including nutrients such as saturated fats and carbohydrates (Valdearcos et al., 2014;
132 Nadjar, et al., 2017; Leyroll, Laye & Nadjar, 2019; Butler et al., 2020). Moreover, activation of
133 microglia alone is sufficient to stimulate food intake and promote weight gain in adult mice, and
134 perturbations that block activation of microglia reduce the metabolic disruption associated with
135 neuroinflammation (Valdearcos et al., 2017; Rosin et al., 2018; Sun et al., 2023). Because of
136 their established role as nutrient-sensing sentinels of hypothalamic neuroinflammation, and
137 their documented participation in neural development (Stevens et al., 2007; Schafer et al.,
138 2012; Stephan et al., 2012), microglia have been proposed as possible mediators of
139 developmental programming caused by nutritional perturbations (Rosin and Kurrasch, 2019;
140 Folick et al., 2021).

141
142 Evidence from several of lines of investigation indicate that microglia have multiple roles in
143 brain development (Schwarz and Bilbo 2009; Tremblay et al., 2011; Miyamoto et al., 2016; Li
144 et al., 2019). Although microglia were initially thought to remain quiescent until activation by
145 neuroinflammation, (Nakajima & Kohsaka, 2001; Nikolic & Tan, 2005) in vivo imaging
146 experiments in the cerebral cortex demonstrated continual activity of their cellular processes,
147 which actively survey their local environment (Stowell et al., 2018), including direct contact with
148 axons and dendrites (Wake et al., 2009; Schafer et al., 2013). In addition to impacting neuronal
149 number and initial formation of neural circuits, microglia are thought to play an important role in
150 synaptic refinement through selective elimination of synapses, a process termed synaptic
151 pruning (Paolicelli et al., 2011; Schafer et al., 2012; Hong, Dissing-Olesen & Stevens, 2016).
152 Thus far, the majority of microglial developmental studies have focused on their role in cortical
153 or hippocampal circuits. However, transcriptional profiling suggests a great deal of regional
154 and temporal variation in microglial cell type and activity (Hammond et al., 2019; Masuda et al.,
155 2020; Young et al., 2021), and the effects of dietary interventions have largely focused on the
156 ARH. Here we used Iba1 immunostaining to visualize and measure morphological changes in
157 microglial morphology in the PVH of offspring exposed to MHFD and compared these effects
158 with those observed in the ARH and bed nuclei of the stria terminalis (BST), a limbic target of
159 AgRP neurons. We also used genetically targeted axonal labeling of AgRP neurons to directly
160 visualize cellular interactions between microglia and labeled AgRP terminals in the PVH and
161 ARH to determine if MHFD stimulates synaptic pruning in these regions. The results
162 demonstrate regionally specific changes to microglia in the PVH of MHFD offspring that are
163 temporally restricted to the period when AgRP neurons innervate the PVH. In addition, the
164 axon labeling experiments confirm a significant decrease in AgRP innervation of the PVH in
165 MHFD offspring, and for the first time provide direct evidence of microglial-mediated synaptic
166 pruning of AgRP terminals in the hypothalamus. Microglial depletion experiments determined
167 that the significant decrease in AgRP innervation of the PVH observed in MHFD offspring

168 requires normal densities of microglia, and that microglia are required for the weight gain seen
169 in offspring of MHFD dams at weaning. However, we did not detect a significant effect of
170 MHFD on the degree of synaptic pruning in the PVH, suggesting an alternative microglial
171 signaling mechanism yet to be identified.

172

173 **2 Results**

174

175 **2.1 Microglia exhibit morphological changes in the PVH in response to MHFD during** 176 **postnatal development.**

177

178 To assess the impact of MHFD on microglia in the brains of postnatal mice, we used Iba1
179 immunohistochemistry and confocal microscopy to visualize the distribution and morphology of
180 microglial cells in the PVH. Discrete regions of interest were imaged and a 3D modeling
181 analysis pipeline was used to measure structural changes in microglia (Figure 1Ai-iii). Although
182 there was no apparent difference between the density of microglia in the PVH of MHFD and
183 NCD offspring at P16 (Figure 1J), the overall size of microglia in the PVH of MHFD offspring
184 was significantly greater, compared to that of NCD mice (Figure 1B, C). The enhanced size of
185 microglia in the MHFD offspring corresponded to an 87% increase in overall process length
186 and a 44% increase in branching complexity (Figure 1F, G). Additionally, the volume of
187 microglial cells (volume of cell body and processes) and the spatial territory they occupy was
188 nearly doubled in MHFD offspring (Figure 1H-I). These morphological changes appeared to be
189 transient because both the density and size of microglia (process length and complexity) were
190 reduced in postweaning mice perfused on P30 (Figure 1D-G). We also assessed the density of
191 AgRP terminals in the same regions of interest in the PVH and confirmed that their density is
192 significantly lower in the brains of MHFD offspring compared with that of NCD controls (Figure
193 1K), as suggested by data published previously (Vogt et al. 2014). Taken together, these
194 results suggest that exposure to MHFD has a profound effect on the morphology of microglia
195 that is consistent with enhanced activity and surveillance of their immediate microenvironment.
196 Furthermore, the effects of MHFD on microglial morphology in the PVH of offspring display
197 both temporal and regional specificity, which correspond to a decrease in the density of AgRP
198 inputs to the PVH.

199

200

201

202 **2.2 Microglia do not exhibit morphological changes in the ARH or BST in response to** 203 **MHFD exposure during postnatal development.**

204

205 The ARH houses the cell bodies of AgRP neurons, and their number is established primarily
206 during prenatal development (Ishii & Bouret 2012). We evaluated microglia morphology in the
207 ARH of postnatal mice by using the same 3D modeling pipeline shown in Figure 1. In sharp
208 contrast to our findings in the PVH, the number and size of microglia in the ARH were not
209 significantly different in NCD and MHFD offspring at P16 (Figure 2A, B; 2E, F). By P30, there
210 was a 67% increase in process length compared to their P16 counterparts, but no significant
211 difference in microglial morphology in the ARH detected between treatment groups (Figure A-
212 l). The volume of microglial cells, as well as the spatial territory they occupy, also increased
213 between P16 and P30 (Figure 2G-H), but the number of microglia visualized was reduced by

214 nearly half (Figure 2I). We also measured numbers of AgRP neuronal cell bodies in the ARH in
215 brains derived from NCD and MHFD offspring and confirmed that the number of AgRP
216 neurons in the ARH are also resistant to MHFD exposure (Figure 2J). In addition, we
217 evaluated microglia and AgRP terminals in the anterolateral part of the BST, an
218 extrahypothalamic target of AgRP neurons innervated during the lactational period (Bouret,
219 Draper and Simerly, 2004a; Cansell et al., 2012; Barbier et al., 2021). As was found for the
220 ARH, neither the number nor size of microglia in the BST were significantly different between
221 NCD and MHFD offspring at P16 or P30 (Figure 3A-D; 3E-I). Similarly, the density of AgRP
222 terminals in the same region of interest was not affected by MHFD exposure (Figure 3J). By
223 P30 the number of AgRP terminals in the BST increased by 61% compared to their P16
224 counterparts (Figure 3J). Taken together, these data suggest that microglia in the ARH and
225 BST are resistant to the increases in cellular complexity that occur in the PVH of MHFD
226 offspring, suggesting a notable degree of spatial specificity in the role of hypothalamic
227 microglia during postnatal development.

228

229

230 **2.3 Microglia are required for changes in AgRP terminal density in PVH and body weight** 231 **associated with MHFD exposure**

232

233 To determine if microglia are required for the observed changes in AgRP inputs to the PVH of
234 MHFD offspring, we depleted microglia during the lactation period. The colony-stimulating
235 factor-1 receptor inhibitor (CSF1R) PLX5622 was administered daily via intraperitoneal
236 injections between P4-P21. These postnatal treatments resulted in a significant decrease in
237 microglia in the PVH at the time of weaning (Figure 4A-B; Figure 4G) that appeared to be
238 widespread throughout the rostral forebrain. Notably, the PLX5622 treatments blocked the
239 reduction in AgRP fiber density observed in the medial dorsal parvicellular part of the PVH
240 (PVHmpd) of vehicle-treated MHFD offspring to a level that was comparable to that of NCD
241 offspring (Figure 4C-F; quantified in 4H). In contrast, MHFD exposure did not affect the density
242 of AgRP fibers in the lateral posterior magnocellular compartment of the PVH (PVHpmi) and
243 no significant difference in AgRP fiber density was detected between MHFD offspring treated
244 with either PLX or vehicle (Figure 4C-F; 4J), suggesting target specificity for the microglia
245 mediated effects on development of AgRP inputs to the PVHmpd.

246

247 Depletion of microglia also appeared to protect against the increase in body weight normally
248 observed in MHFD mice. In keeping with previously published results (Vogt et al. 2014), the
249 weight of vehicle treated MHFD animals was significantly greater (24%), compared with that of
250 NCD animals (Figure 4I). However, MHFD mice treated with PLX5622 during lactation
251 exhibited significantly lower weights at P21 compared to those of vehicle-treated MHFD
252 animals. Taken together, these findings suggest that microglia mediate target-specific effects
253 of MHFD exposure on the innervation of the PVH by AgRP neurons, and that microglia play a
254 role in mediating the effects of MHFD on body weight.

255

256 **2.4 Engulfment of AgRP terminals by microglia in the PVH and the ARH**

257

258 Microglia are thought to impact development of neuronal connections through an active
259 engulfment mechanism and the lysosomal associated membrane protein CD68 has

260 been implicated in this process. Here, we used immunohistochemistry to visualize the
261 presence of in Iba1-labeled microglia in mice with genetically targeted labeling of AgRP
262 terminals. Many apparent contacts between microglial processes and AgRP terminals in
263 the PVH and ARH were observed at P16 and P30, including internalized AgRP
264 terminals (Figure 5A-L). However, the extent of internalization did not appear to be
265 influenced by MHFD exposure; there were no significant differences between
266 internalized AgRP terminals in MHFD and NCD offspring at P16, in either the PVH or
267 ARH (Figure 5M, O). Similarly, we did not detect a statistically significant difference in
268 microglial CD68 levels in the PVH between diet groups at P30 (Figure 5N). Consistent
269 with previous reports, (Wong et al. 2005; Hart et al. 2012) the density of CD68 labeled
270 profiles nearly doubled in the PVH between P16 and P30 (Figure 5N), as microglia
271 become more phagocytic with age. CD68 staining also increased in the ARH between
272 P16 and P30 (Figure 5P), supporting the notion that microglia increase their phagocytic
273 capacity with age. Nevertheless, our analysis demonstrates that microglia interact
274 directly with AgRP terminals, with clear evidence of engulfment. MHFD exposure does
275 not appear to promote microglia-mediated engulfment, at least not in the specific PVH
276 and ARH domains examined.

277

278 **3 Discussion**

279

280 It is well established that microglia are responsive to HFD exposure in adult rodents (Thaler et
281 al., 2012; Morari et al., 2014; Valdearcos et al., 2014; Baufeld et al., 2016; Valdearcos et al.,
282 2017) and multiple lines of evidence support an important role for microglia in mediating key
283 aspects of neural circuit development (Checchin et al., 2006; Hoshiko et al. 2012; Li et al.,
284 2012; Hagemeyer et al., 2017). Here we demonstrate that microglia are required for significant
285 elevations in body weight that emerge from postnatal exposure to HFD and are associated
286 with a sustained decrease in the density of afferents from AgRP neurons to the PVH in
287 offspring. Exposure to MHFD caused distinct morphological changes to microglia that are
288 consistent with enhanced activity, which were observed in the PVH, but not the ARH or BST.
289 Moreover, the morphological changes to microglia observed appear to be primarily limited to
290 the critical period for development of AgRP inputs to PVH neurons in MHFD offspring.
291 Although our results demonstrate that microglia engage in engulfment of AgRP terminals in the
292 PVH during development, synaptic pruning by microglia does not appear to represent the
293 cellular mechanism mediating the effects of MHFD exposure on innervation of the PVH by
294 AgRP neurons.

295

296 **3.1 A Role for Microglia in Mediating Body Weight Changes Observed in MHFD**

297 **Offspring**

298

299 Maternal high fat diet exposure during a period that extends across both gestation and
300 lactation causes offspring to have increased body weight, fat content and susceptibility to diet-
301 induced obesity (Samuelsson et al., 2008; Masuyama et al., 2014; Gomes et al., 2018). In
302 contrast to the more variable impact of maternal HFD exposure just during gestation, limiting
303 HFD exposure to the postnatal period, which corresponds to lactation, when mice derive their
304 nutrition primarily from milk, reliably predisposes adult mice to obesity. Feeding pregnant dams
305 HFD during the week prior to parturition leads to either increased body weight in offspring

306 (Akhaphong et al., 2021) or no significant effect (Sun et al, 2012; Vogt et al., 2014), suggesting
307 that MHFD plays a dominant role in specifying metabolic phenotype later in life (Sun et al.,
308 2012; Vogt et al. 2014). In the present study, global depletion of microglia with the CSF1R
309 inhibitor PLX5622 blocked the ability of MHFD to increase body weight in mice at P21,
310 indicating that microglia may mediate metabolic changes caused by MHFD exposure that are
311 apparent as early as weaning. A previous study that used intragastric administration of
312 PLX3397 to neonatal mice reported enhanced food intake in the offspring during lactation (Sun
313 et al., 2023). Notably, these mice were not derived from MHFD dams. Microglial depletion with
314 PLX5622 in adult mice was found to mitigate the effects of HFD exposure (Rosin et al., 2018)
315 and our results indicate that microglia may function similarly in offspring during postnatal life to
316 effect changes in body weight, even if the maternal HFD exposure is restricted to the lactation
317 period. Further studies are required to define the long-term metabolic profile resulting from
318 developmental microglial manipulations. However, given the abundant literature on sustained
319 impact of MHFD on metabolic phenotype, enduring disruptions are likely. It should be noted
320 that PLX5622 treatment is not spatially limited to the PVH or ARH, leaving open the possibility
321 that the effects of microglial depletion on body weight occur outside of these nuclei, or are due
322 to collective activation of microglia in multiple components of feeding circuitry (Green, Crasper
323 and Hohsfield, 2020). Localization of the specific site of action for microglial specification of
324 mature body weight during development will require utilization of specific markers for
325 hypothalamic microglia that account for regional and phenotypic heterogeneity, perhaps
326 through intersectional genetic methods and combinatorial pharmacology (Hammond et al.,
327 2019; Kim et al., 2021).

328

329 **3.2 MHFD Induces Spatially Limited Changes in Microglial Morphology**

330

331 Morphological changes in microglia have been reported in response to a variety of
332 environmental exposures. In the hypothalamus, adult mice fed a high fat diet show both
333 proliferation and changes in process length and complexity (Thaler et al., 2012; Valdearcos et
334 al, 2017). In our studies, MHFD exposure caused a marked increase in the overall size of
335 microglia in the PVH related to increases in both the length and branching complexity of Iba-1-
336 stained cellular processes. This increase in the territory occupied by microglia in the PVH was
337 not accompanied by an increase in microglial number, nor were numbers of microglia affected
338 in the PVH by MHFD exposure. However, in contrast to the PVH, changes in microglial
339 morphology were not observed in the ARH in response to MHFD, although we did observe an
340 overall increase in process length in the ARH between P16 and P30 of both MHFD and NCD
341 mice. This finding is consistent with previously published reports on microglial maturation (Sun
342 et al., 2023). The spatially restricted enhancement of microglial activation in the PVH resulting
343 from MHFD exposure appears to contribute to an expansion of parenchymal territory surveilled
344 by PVH microglia, as reflected in the volume measurements accomplished with geometrical
345 modeling of process length and complexity. This interpretation is supported by *in vitro* and *in*
346 *vivo* observations of enhanced process extension and increased neuronal interactions
347 resulting from inflammatory activation of microglia (Wake et al., 2009; Schafer et al., 2013;
348 Dissing-Olesen et al., 2014; Stowell et al., 2018; Bolton et al., 2022).

349

350 As in the ARH, we did not observe comparable changes in microglial morphology in the BST,
351 an extrahypothalamic target of AgRP neurons innervated during the lactation period (Cansell

352 et al., 2012; Barbier et al., 2021). These observations underscore the remarkable molecular
353 heterogeneity of microglial phenotypes that appear to occupy various hypothalamic niches
354 during development, and which may have equally diverse developmental roles and responses
355 to environmental signals (Bilbo and Schwarz, 2012; Frost and Schafer, 2016; Li and Barres,
356 2018; Ngozi and Bolton, 2022). Moreover, the observed morphological changes in the PVH
357 caused by MHFD appear to be transient as there no significant differences in microglial
358 processes by P30, and the density of microglial cells in the PVH was significantly reduced in
359 the older mice, suggesting a decline in overall activity. Temporal alignment of these
360 morphological events with the critical period for development of AgRP projections to the PVH
361 suggests a possible role for microglia linking nutrition with specification of axonal targeting
362 (Kamitakahara et al., 2018).

363

364 **3.3 Microglia Mediate Impaired Innervation of the PVH by AgRP Neurons**

365

366 AgRP neuronal projections develop primarily during the first two weeks of life, which
367 corresponds to a critical period for the neurotrophic action of leptin on axonal outgrowth and
368 targeting of AgRP inputs to distinct components of the PVH (Simerly, 2008; Elson and Simerly,
369 2015). Exposure to MHFD during this critical developmental window permanently impairs
370 AgRP projections to the PVH, DMH and LH (Vogt et al., 2014) that are associated with
371 increased body weight in adulthood. Here we confirm that MHFD impairs innervation of the
372 PVH, and this defect was apparent as early as P16. The PVH is innervated by AgRP neurons
373 between P8 and P10 (Bouret, Draper and Simerly, 2004a). We found that depletion of
374 microglia with PLX5622 between P4 and P21, a period that aligns not only with AgRP
375 innervation of the PVH but also with maximum changes in microglial morphology, blocked the
376 effects of MHFD on AgRP terminals in the PVH. However, this partial rescue of innervation
377 appeared to be limited to the PVHmpd, suggesting that there is a profound regional
378 specialization in the activity of microglia in the PVH. We did not observe a change in AgRP
379 innervation of the BST in MHFD offspring that mirrored the changes seen in the PVH of the
380 same animals, further supporting the conclusion that microglia display significant spatial
381 heterogeneity in mediating site-specific alterations in AgRP axon targeting.

382

383 Microglia are known to impact a variety of developmental events, including alterations in cell
384 number through programmed cell death or neurogenesis, as well as axonal targeting and
385 remodeling of neural circuits (Frost and Schafer, 2016; Li and Barres 2018). It is unlikely that
386 the impaired innervation of the PVH observed in MHFD offspring is due to a reduction in the
387 number of AgRP neurons in the ARH (Vogt et al, 2014; Valdearcos et al., 2017). Sun and
388 colleagues reported that microglial depletion during postnatal life actually increases numbers
389 of AgRP neurons, as well as enhances local densities of AgRP fibers in the ARH, possibly
390 through enhanced formation of perineuronal nets (Sun et al., 2023). However, changes in
391 AgRP targets outside of the ARH were not assessed. Depletion of microglia during gestation
392 causes a significant decrease in the number of proopiomelanocortin (POMC) neurons in the
393 ARH and leads to an acceleration of weight gain (Rosin et al., 2018), consistent with
394 neurogenesis of ARH neurons occurring in mid gestation and being susceptible to nutritional
395 impacts during embryonic life (Ishii and Bouret, 2012; Elson and Simerly, 2015). Interestingly,
396 genetic deletion of leptin receptors from myeloid cells reduced numbers of POMC neurons in
397 the ARH, suppressed POMC innervation of the PVH, and decreased microglial process

398 complexity (Gao et al., 2017). Taken together, these results suggest that leptin signaling in
399 microglia may act at the level of the ARH to promote growth of AgRP projections to the PVH,
400 while MHFD activates microglia in the PVH to specify patterns of AgRP afferents that are not
401 only regionally specific, but also target discrete domains of the PVH. However, whether
402 microglia inhibit synaptogenesis or are involved in synaptic refinement through an alternative
403 regressive mechanism will require further investigation.

404

405 **3.4 Microglia in PVH Participate in Synaptic Pruning**

406

407 Microglia play an important role in synaptic pruning, a process whereby synapses that form
408 early in development are eliminated as others are strengthened and maintained (Katz and
409 Shatz, 1996; Sanes and Lichtman, 1999; Frost and Schafer 2016; Li and Barres, 2018).
410 Although this process has been studied most extensively in somatosensory cortex (Miyamoto
411 et al., 2016), hippocampus (Paolicelli et al., 2011; Wang et al. 2020) and the visual system
412 (Tremblay et al., 2010; Schafer et al., 2012), there is clear evidence for involvement of
413 microglia in synaptic pruning of immunolabeled glutamatergic terminals associated with
414 corticotropin releasing hormone neurons in the PVH (Bolton et al., 2022). In the present study,
415 we used AgRP axonal labeling to provide evidence that microglia in the PVH participate in
416 synaptic pruning of AgRP/GABAergic synapses during the critical period for PVH innervation,
417 and when PVH microglia exhibit high levels of process extension. The lysosomal marker CD68
418 was colocalized with internalized AgRP terminals in PVH microglia, and although elevated at
419 P30, there were no differences between offspring of MHFD and NCD dams. Additionally, we
420 did not find a significant difference between the density of engulfed AgRP terminals in the PVH
421 of MHFD offspring at either P16 or P30. However, enhanced engulfment of AgRP terminals in
422 MHFD offspring may occur at a later point in development. It is also possible that the
423 synaptophysin-tdTomato axonal label may have been lost from pruned synapses during
424 engulfment. A more probable interpretation is that PVH microglia participate in synaptic
425 refinement through other cellular mechanisms, including microglial release of secreted factors
426 such as IL6 (Kim, Copperi, and Diano, 2024) or microglial derived BDNF (Parkhurst et al.,
427 2013). Additional investigation is required to resolve this question.

428

429 **4 Conclusions**

430

431 MHFD causes elevated levels of saturated carbohydrates and fats in milk (Gorski et al., 2006;
432 Vogt et al., 2014; Calvo-Lerma et al., 2022). The resulting overnutrition resulting from exposure
433 to this enhanced diet is thought to underly the propensity towards obesity observed in offspring
434 later in life (Skowronski, Leibel and Leduc, 2023). Although microglia are likely mediators of
435 multiple neurobiological events influencing how hypothalamic circuits function during regulation
436 of energy balance, the precise signaling mechanisms remain ill defined. There may be
437 common molecular mechanisms underlying the effects of HFD exposure on microglial
438 activation in adults and those occurring during postnatal development, but how these signaling
439 events exert a lasting impact on the organization and function of feeding circuitry has not been
440 defined. The results presented here clearly demonstrate an important role for microglia,
441 specifically in the PVH, on sculpting the density of AgRP inputs to the PVH that is not only
442 spatially restricted, but also aligned temporally with synaptogenesis in the PVH. Furthermore,
443 PVH microglia clearly interact directly with AgRP afferent axons during this critical period and

444 appear to be refined through engulfment by microglia. However, synaptic pruning does not
 445 appear to be sufficient to affect the significant reduction in AgRP innervation of PVH neurons
 446 observed following MHFD exposure, suggesting involvement of additional microglial signaling
 447 mechanisms that are not only important for specifying patterns of innervation of the PVH by
 448 AgRP neurons, but may also contribute more broadly to developmental programming of
 449 metabolic phenotype.

450

451 5 Materials and Methods

452

453 5.1 Key Resources Table

Reagent type or resource	Designation	Source or reference	Identifiers	Additional information
Genetic reagent (<i>M. musculus</i>)	AgRP-IRES-Cre	Jackson Laboratory	Stock #: 012899 RRID: IMSR_JAX:012899	MGI ID: J:140858
Genetic reagent (<i>M. musculus</i>)	Synaptophysin-tdTomato	Jackson Laboratory	Stock #: 012570 RRID: IMSR_JAX:012570	MGI ID: J:170755
Antibody	Rabbit polyclonal anti-Iba1	FUJIFILM Wako Shibayagi	Cat. #: 019-19741 RRID: AB_839504	IHC (1:2000)
Antibody	Rat monoclonal anti-CD68 [FA-11]	Abcam	Cat. #: ab53444 RRID: AB_869007	IHC (1:500)
Antibody	Donkey polyclonal anti-rabbit Alexa Fluor 488	ThermoFisher Scientific	Cat. #: A32790 RRID: AB_2762833	IHC (1:500)
Antibody	Donkey polyclonal anti-rat Alexa Fluor 647	ThermoFisher Scientific	Cat. #: A48272 AB_2893138	IHC (1:500)
Pharmacological Inhibitor	PLX5622 hemifumarate, CSF1R inhibitor	MedChemExpress	Cat. # HY114153A	
Software, Algorithm	Imaris	Bitplane	V9.5	
Software, Algorithm	GraphPad Prism	Prism	Prism 7	

454

455

456 5.2 Animal Care

457 Transgenic mice expressing IRES-Cre recombinase under the control of the AgRP promoter,
 458 AgRP-Cre mice (AgRP-IRES-Cre Stock no: 012899; MGI:J:140858) and mice expressing the
 459 cre-dependent fluorescent reporter synaptophysin-tdTomato (SynTom mice; Ai34D-Rosa-
 460 CAG-LSL-Synaptophysin-tdTomato-WPRE; stock number: 012570; MGI:J:170755) were
 461 obtained from the Jackson Laboratory (Bar Harbor, ME) and maintained in our colony at

462 Vanderbilt University. Wild-type C57BL/6J mice (stock number: 000664) were also obtained
463 from The Jackson Laboratory. To visualize AgRP inputs, AgRP-Cre mice were crossed with
464 SynTom mice to generate AgRP-Cre::SynTom mice, as described previously (Biddinger, et.al.,
465 2020).

466
467 All animal care and experimental procedures were performed in accordance with the
468 guidelines of the National Institutes of Health and the Institutional Care and Use Committee of
469 Vanderbilt University. Mice were housed at 22°C on a 12:12 h light:dark cycle (lights on at 6:00
470 a.m.: lights off at 6:00 p.m.). Mice were provided ad libitum access to a standard chow diet
471 (PicoLab Rodent Diet 20 #5053), unless otherwise specified.

472
473 To generate offspring of dams exposed to HFD during lactation (MHFD) mice had ad libitum
474 access to normal chow (PicoLab Rodent Diet, 5053LabDiet: 25% protein; 62% carbohydrates;
475 13% fat; 4 kcal/g energy density) during mating. On the first postnatal day (P1) all litters were
476 adjusted to 7 pups to normalize nutrition and dams were switched to either high fat diet (HFD)
477 (Research Diets D12451: 20% protein; 35% carbohydrate; 45% fat; 4.7 kcal/g energy density)
478 or kept on normal chow diet (NCD). The dams remained on either HFD or NCD through
479 lactation, and at weaning the offspring were switched to a normal chow diet, regardless of
480 lactation diet condition.

481

482 **5.3 PLX5622 Microglia Depletion**

483 To reduce microglia during postnatal development (P4-P21) mice were treated with PLX5622,
484 a colony stimulating factor 1 receptor (CSF1R) inhibitor or with DMSO vehicle via
485 intraperitoneal injection (Riquier et al. 2020). Briefly, PLX5622 hemifurate solid (Cat.
486 #HY114153A MedChemExpress, Monmouth Junction, NJ, USA) was suspended in dimethyl
487 sulfoxide at a concentration of 172 mg/ml. The injection working solution was prepared to
488 include 20% Kolliphor RH40 diluted in PBS, which resulted in doses with a 6.5mg/ml PLX5622
489 concentration and injection concentration of 15 mg/kg. IP injections were given once daily from
490 P4 to P21 and injection dose was determined by each animal's body weight at time of
491 injection.

492

493 **5.4 Immunohistochemistry**

494 Mice were perfused at P16 and P30 and processed for immunofluorescence by using an
495 antibody to Iba-1 (1:2000; FUJIFILM Wako Pure Chemicals, Osaka, Japan) to visualize
496 microglia and an antibody to CD68 (1:500; Abcam, Cambridge, MA, USA) to assess
497 phagocytic capacity of the microglia. Mice were first anesthetized with tribromoethanol (TBE)
498 and then perfused transcardially with cold 0.9% saline, followed by cold fixative (4%
499 paraformaldehyde in borate buffer, pH 9.5) for 10 minutes. Brains were then removed from
500 skull and postfixed in the same fixative overnight. Brains were then cryoprotected overnight in
501 a 20% sucrose solution before being frozen in optimal temperature cutting compound (Sakura
502 Finetek Inc., Torrance, CA) and sectioned on a freezing stage sliding microtome at 30µm.
503 Free-floating brain sections were rinsed in KPBS and then incubated in blocking buffer
504 containing 2% normal donkey serum and 0.3% Triton-X overnight at 4°C. Sections were
505 transferred to primary antibody incubation for 48hr with rabbit anti-Iba-1 antibody and rat anti-
506 CD68 antibody. Following primary antibody incubation, sections were rinsed several times in
507 KPBS, incubated for an hour at room temperature in blocking buffer containing secondary

508 antibodies against rabbit and rat (raised in donkey) conjugated with Alexa-Fluor fluorochromes
509 (1:500; Life Technologies, Carlsbad, CA, USA), mounted onto charged microscope slides and
510 coverslipped using ProLong antifade mounting medium (Life Technologies, Carlsbad, CA,
511 USA).

512
513 **5.5 Image Acquisition and Analysis**
514 Sections through the PVH, ARH, and BST were examined on a laser scanning confocal
515 microscope (Zeiss 800) and cytoarchitectonic features of the nuclei were visualized with
516 Hoescht 33342, and used to define matching regions of interest (ROI) for quantitative analysis.
517 Confocal image stacks were collected for each ROI through the entire thickness of the region
518 at a frequency of 0.1 μ m using the 40x objective. Imaris visualization software (Bitplane V9.5,
519 Salisbury Cove, ME, USA) was used to create 3D reconstructions of each multichannel set of
520 images.

521
522 3D reconstructions of microglia based on Iba-1 immunofluorescence were made using made
523 using Imaris (Bitplane, v9.5). Profiles were skeletonized automatically by using the Filaments
524 tool in order to quantify changes in microglia structure. Sholl analysis (Geoffroy et al., 2014),
525 was performed on the skeletonized structures to determine complexity of branching of
526 microglial processes. Briefly, 3D concentric spheres are drawn around the microglia skeleton
527 and each contact point between microglial process and sphere is counted as 1 level of
528 branching. The higher the number of contacts, the higher complexity of branching in the
529 microglia. 3D reconstructions of the microglia were also evaluated for length of processes as
530 well as cell volume and the area that is occupied. To evaluate the 3D space occupied by each
531 microglial cell, a polyhedron was drawn around the microglia by using the built-in Convex Hull
532 function under Filaments, which is used to calculate volume of the polyhedron automatically,
533 accounting for the 3D space around the microglia.

534
535 In order to assess cellular interactions between AgRP terminals and microglia, the 3D
536 renderings were used to determine level of contact by using a MATLAB script to automate the
537 analysis. Both channels were subjected to background subtraction and Gaussian filtering. The
538 automatic threshold calculated was based on k-means statistical methods and was used in the
539 majority of analyses. The AgRP terminals were reconstructed as “spots” of 0.8 μ m diameter
540 (corresponding to the largest measured size) and their total number was automatically
541 calculated. Briefly, the automatic detection algorithm applies a 3D Mexican hat filter using the
542 spot size and then locates the spot centroid at the local maxima of the filtered image. The
543 number of spots located at no more than 1 μ m from the microglia surface was automatically
544 determined and indicated as a contact point. Next, spots that were determined to be less than
545 0.5 μ m away from internal microglial surfaces were determined to be internalized by the
546 microglia and counted as engulfed. CD68 levels were determined using automated analysis to
547 create 3D renderings and their volume computed.

548
549 **5.6 Statistical Analyses**
550 Data are presented as the mean values \pm SEM. Descriptive statistics and unpaired t-tests were
551 used to compute group differences using GraphPad Prism software (GraphPad Software, San
552 Diego, CA). P-value less than 0 .05 were considered significant.

553

554 **Acknowledgments**

555
556 We thank the members of the Simerly Lab for comments and discussion on early versions of
557 this manuscript. This work was supported by NIH grants R01DK106476 (RBS) and
558 T32DK07563 (HNM-R).

560 **Author Contributions**

561
562 HNM-R and RBS conceived of this research and designed experiments. HNM-R conducted
563 experiments with technical support from JEB and MNB. HNM-R and JEB analyzed data and
564 prepared figures. HNM-R and RBS wrote the manuscript and all authors participated in editing
565 the manuscript.

567 **References**

- 568
569 Akhaphong, B., Gregg, B., Kumusoglu, D., Jo, S., Singer, K., Scheys, J., DelProposto, J.,
570 Lumeng, C., Bernal-Mizrachi, E., & Alejandro, E. U. (2022). Maternal High-Fat Diet During
571 Pre-Conception and Gestation Predisposes Adult Female Offspring to Metabolic
572 Dysfunction in Mice. *Frontiers in Endocrinology*, 12, 780300.
573 <https://doi.org/10.3389/fendo.2021.780300>
- 574 Andersen, L. G., Holst, C., Michaelsen, K. F., Baker, J. L., & Sørensen, T. I. A. (2012). Weight
575 and weight gain during early infancy predict childhood obesity: a case-cohort study.
576 *International Journal of Obesity*, 36(10), 1306–1311. <https://doi.org/10.1038/ijo.2012.134>
- 577 Barbier, M., González, J. A., Houdayer, C., Burdakov, D., Risold, P., & Croizier, S. (2021).
578 Projections from the dorsomedial division of the bed nucleus of the stria terminalis to
579 hypothalamic nuclei in the mouse. *Journal of Comparative Neurology*, 529(5), 929–956.
580 <https://doi.org/10.1002/cne.24988>
- 581 Baufeld, C., Osterloh, A., Prokop, S., Miller, K. R., & Heppner, F. L. (2016). High-fat diet-
582 induced brain region-specific phenotypic spectrum of CNS resident microglia. *Acta*
583 *Neuropathologica*, 132(3), 361–375. <https://doi.org/10.1007/s00401-016-1595-4>
- 584 Betley, J. N., Xu, S., Cao, Z. F. H., Gong, R., Magnus, C. J., Yu, Y., & Sternson, S. M.
585 (2015). Neurons for hunger and thirst transmit a negative-valence teaching
586 signal. *Nature*, 521(7551), 180-185. <https://doi.org/10.1038/nature14416>
- 587 Biddinger, J. E., Lazarenko, R. M., Scott, M. M., & Simerly, R. (2020). Leptin suppresses
588 development of GLP-1 inputs to the paraventricular nucleus of the hypothalamus. *ELife*, 9,
589 e59857. <https://doi.org/10.7554/elife.59857>
- 590 Bilbo, S. D., & Schwarz, J. M. (2009). Early-Life Programming of Later-Life Brain and Behavior:
591 A Critical Role for the Immune System. *Frontiers in Behavioral Neuroscience*, 3, 14.
592 <https://doi.org/10.3389/neuro.08.014.2009>

- 593 Bilbo, S. D., & Schwarz, J. M. (2012). The immune system and developmental programming of
594 brain and behavior. *Frontiers in Neuroendocrinology*, 33(3), 267–286.
595 <https://doi.org/10.1016/j.yfrne.2012.08.006>
- 596 Bolton, J. L., Short, A. K., Othy, S., Kooiker, C. L., Shao, M., Gunn, B. G., Beck, J., Bai, X.,
597 Law, S. M., Savage, J. C., Lambert, J. J., Belelli, D., Tremblay, M.-È., Cahalan, M. D., &
598 Baram, T. Z. (2022). Early stress-induced impaired microglial pruning of excitatory synapses
599 on immature CRH-expressing neurons provokes aberrant adult stress responses. *Cell*
600 *Reports*, 38(13), 110600. <https://doi.org/10.1016/j.celrep.2022.110600>
- 601 Bouret, S. G., Draper, S. J., & Simerly, R. B. (2004a). Formation of Projection Pathways from
602 the Arcuate Nucleus of the Hypothalamus to Hypothalamic Regions Implicated in the Neural
603 Control of Feeding Behavior in Mice. *The Journal of Neuroscience*, 24(11), 2797–2805.
604 <https://doi.org/10.1523/jneurosci.5369-03.2004>
- 605 Bouret, S. G., Draper, S. J., & Simerly, R. B. (2004b). Trophic Action of Leptin on
606 Hypothalamic Neurons That Regulate Feeding. *Science*, 304(5667), 108–110.
607 <https://doi.org/10.1126/science.1095004>
- 608 Bouret, S., Levin, B. E., & Ozanne, S. E. (2015). Gene-Environment Interactions Controlling
609 Energy and Glucose Homeostasis and the Developmental Origins of Obesity. *Physiological*
610 *Reviews*, 95(1), 47–82. <https://doi.org/10.1152/physrev.00007.2014>
- 611 Bouyer, K., & Simerly, R. B. (2013). Neonatal Leptin Exposure Specifies Innervation of
612 Presympathetic Hypothalamic Neurons and Improves the Metabolic Status of Leptin-
613 Deficient Mice. *The Journal of Neuroscience*, 33(2), 840–851.
614 <https://doi.org/10.1523/jneurosci.3215-12.2013>
- 615 Butler, M. J., Cole, R. M., Deems, N. P., Belury, M. A., & Barrientos, R. M. (2020). Fatty food,
616 fatty acids, and microglial priming in the adult and aged hippocampus and amygdala. *Brain*,
617 *Behavior, and Immunity*, 89, 145–158. <https://doi.org/10.1016/j.bbi.2020.06.010>
- 618 Calvo-Lerma, J., Selma-Royo, M., Hervas, D., Yang, B., Intonen, L., González, S., Martínez-
619 Costa, C., Linderborg, K. M., & Collado, M. C. (2022). Breast Milk Lipidome Is Associated
620 With Maternal Diet and Infants' Growth. *Frontiers in Nutrition*, 9, 854786.
621 <https://doi.org/10.3389/fnut.2022.854786>
- 622 Cansell, C., Denis, R. G. P., Joly-Amado, A., Castel, J., & Luquet, S. (2012). Arcuate AgRP
623 neurons and the regulation of energy balance. *Frontiers in Endocrinology*, 3, 169.
624 <https://doi.org/10.3389/fendo.2012.00169>
- 625 Cansell, C., Stobbe, K., Sanchez, C., Thuc, O. L., Mosser, C., Ben-Fradj, S., Leredde, J.,
626 Lebeaupein, C., Debayle, D., Fleuriot, L., Brau, F., Devaux, N., Benani, A., Audinat, E.,
627 Blondeau, N., Nahon, J., & Rovère, C. (2021). Dietary fat exacerbates postprandial
628 hypothalamic inflammation involving glial fibrillary acidic protein-positive cells and microglia
629 in male mice. *Glia*, 69(1), 42–60. <https://doi.org/10.1002/glia.23882>

- 630 Checchin, D., Sennlaub, F., Levavasseur, E., Leduc, M., & Chemtob, S. (2006). Potential Role
631 of Microglia in Retinal Blood Vessel Formation. *Investigative Ophthalmology & Visual*
632 *Science*, 47(8), 3595. <https://doi.org/10.1167/iovs.05-1522>
- 633 Chen, Y., Lin, Y. C., Kuo, T. W., & Knight, Z. A. (2015). Sensory detection of food
634 rapidly modulates arcuate feeding circuits. *Cell*, 160(5), 829-841.
635 <https://doi.org/10.1016/j.cell.2015.01.033>
- 636 Collaboration, P. S., Whitlock, G., Lewington, S., Sherliker, P., Clarke, R., Emberson, J.,
637 Halsey, J., Qizilbash, N., Collins, R., & Peto, R. (2009). Body-mass index and cause-
638 specific mortality in 900 000 adults: collaborative analyses of 57 prospective studies.
639 *Lancet*, 373(9669), 1083–1096. [https://doi.org/10.1016/s0140-6736\(09\)60318-4](https://doi.org/10.1016/s0140-6736(09)60318-4)
- 640 Dissing-Olesen, L., LeDue, J. M., Rungta, R. L., Hefendehl, J. K., Choi, H. B., & MacVicar, B.
641 A. (2014). Activation of Neuronal NMDA Receptors Triggers Transient ATP-Mediated
642 Microglial Process Outgrowth. *The Journal of Neuroscience*, 34(32), 10511–10527.
643 <https://doi.org/10.1523/jneurosci.0405-14.2014>
- 644 Elson, A. E., & Simerly, R. B. (2015). Developmental specification of metabolic circuitry.
645 *Frontiers in Neuroendocrinology*, 39, 38–51. <https://doi.org/10.1016/j.yfrne.2015.09.003>
- 646 Folick, A., Koliwad, S. K., & Valdearcos, M. (2021). Microglial Lipid Biology in the
647 Hypothalamic Regulation of Metabolic Homeostasis. *Frontiers in Endocrinology*, 12,
648 668396. <https://doi.org/10.3389/fendo.2021.668396>
- 649 Frost, J. L., & Schafer, D. P. (2016). Microglia: Architects of the Developing Nervous System.
650 *Trends in Cell Biology*, 26(8), 587–597. <https://doi.org/10.1016/j.tcb.2016.02.006>
- 651 Gao, Y., Vidal-Itriago, A., Milanova, I., Korpel, N. L., Kalsbeek, M. J., Tom, R. Z., Kalsbeek, A.,
652 Hofmann, S. M., & Yi, C.-X. (2017). Deficiency of leptin receptor in myeloid cells disrupts
653 hypothalamic metabolic circuits and causes body weight increase. *Molecular Metabolism*, 7,
654 155–160. <https://doi.org/10.1016/j.molmet.2017.11.003>
- 655 García-Cáceres, C., Balland, E., Prevot, V., Luquet, S., Woods, S. C., Koch, M., Horvath, T. L.,
656 Yi, C.-X., Chowen, J. A., Verkhatsky, A., Araque, A., Bechmann, I., & Tschöp, M. H. (2019).
657 Role of astrocytes, microglia, and tanycytes in brain control of systemic metabolism. *Nature*
658 *Neuroscience*, 22(1), 7–14. <https://doi.org/10.1038/s41593-018-0286-y>
- 659 Geoffroy, Derecki, N., & Kipnis, J. (2014). Microglial Scholl Analysis. *Protocol Exchange*.
- 660 Gomes, D., Kries, R. von, Delius, M., Mansmann, U., Nast, M., Stubert, M., Langhammer, L.,
661 Haas, N. A., Netz, H., Obermeier, V., Kuhle, S., Holdt, L. M., Teupser, D., Hasbargen, U.,
662 Roscher, A. A., & Ensenauer, R. (2018). Late-pregnancy dysglycemia in obese pregnancies
663 after negative testing for gestational diabetes and risk of future childhood overweight: An
664 interim analysis from a longitudinal mother–child cohort study. *PLoS Medicine*, 15(10),
665 e1002681. <https://doi.org/10.1371/journal.pmed.1002681>

- 666 Gorski, J. N., Dunn-Meynell, A. A., Hartman, T. G., & Levin, B. E. (2006). Postnatal
667 environment overrides genetic and prenatal factors influencing offspring obesity and insulin
668 resistance. *American Journal of Physiology-Regulatory, Integrative and Comparative*
669 *Physiology*, 291(3), R768–R778. <https://doi.org/10.1152/ajpregu.00138.2006>
- 670 Green, K. N., Crapser, J. D., & Hohsfield, L. A. (2020). To Kill a Microglia: A Case for CSF1R
671 Inhibitors. *Trends in Immunology*, 41(9), 771–784. <https://doi.org/10.1016/j.it.2020.07.001>
- 672 Hagemeyer, N., Hanft, K.-M., Akritidou, M.-A., Unger, N., Park, E. S., Stanley, E. R.,
673 Staszewski, O., Dimou, L., & Prinz, M. (2017). Microglia contribute to normal
674 myelinogenesis and to oligodendrocyte progenitor maintenance during adulthood. *Acta*
675 *Neuropathologica*, 134(3), 441–458. <https://doi.org/10.1007/s00401-017-1747-1>
- 676 Hammond, T. R., Dufort, C., Dissing-Olesen, L., Giera, S., Young, A., Wysoker, A., Walker, A.
677 J., Gergits, F., Segel, M., Nemesh, J., Marsh, S. E., Saunders, A., Macosko, E., Ginhoux,
678 F., Chen, J., Franklin, R. J. M., Piao, X., McCarroll, S. A., & Stevens, B. (2019). Single-Cell
679 RNA Sequencing of Microglia throughout the Mouse Lifespan and in the Injured Brain
680 Reveals Complex Cell-State Changes. *Immunity*, 50(1), 253–271.e6.
681 <https://doi.org/10.1016/j.immuni.2018.11.004>
- 682 Hart, A. D., Wyttenbach, A., Perry, V. H., & Teeling, J. L. (2012). Age related changes in
683 microglial phenotype vary between CNS regions: Grey versus white matter differences.
684 *Brain, Behavior, and Immunity*, 26(5), 754–765. <https://doi.org/10.1016/j.bbi.2011.11.006>
- 685 Hong, S., Dissing-Olesen, L., & Stevens, B. (2016). New insights on the role of microglia in
686 synaptic pruning in health and disease. *Current Opinion in Neurobiology*, 36, 128–134.
687 <https://doi.org/10.1016/j.conb.2015.12.004>
- 688 Horvath, T. L., Sarman, B., García-Cáceres, C., Enriori, P. J., Sotonyi, P., Shanabrough, M.,
689 Borok, E., Argente, J., Chowen, J. A., Perez-Tilve, D., Pfluger, P. T., Brönneke, H. S., Levin,
690 B. E., Diano, S., Cowley, M. A., & Tschöp, M. H. (2010). Synaptic input organization of the
691 melanocortin system predicts diet-induced hypothalamic reactive gliosis and obesity.
692 *Proceedings of the National Academy of Sciences*, 107(33), 14875–14880.
693 <https://doi.org/10.1073/pnas.1004282107>
- 694 Hoshiko, M., Arnoux, I., Avignone, E., Yamamoto, N., & Audinat, E. (2012). Deficiency of the
695 Microglial Receptor CX3CR1 Impairs Postnatal Functional Development of Thalamocortical
696 Synapses in the Barrel Cortex. *The Journal of Neuroscience*, 32(43), 15106–15111.
697 <https://doi.org/10.1523/jneurosci.1167-12.2012>
- 698 Ishii, Y., & Bouret, S. G. (2012). Embryonic Birthdate of Hypothalamic Leptin-Activated
699 Neurons in Mice. *Endocrinology*, 153(8), 3657–3667. <https://doi.org/10.1210/en.2012-1328>
- 700 Kamitakahara, A., Bouyer, K., Wang, C., & Simerly, R. (2018). A critical period for the trophic
701 actions of leptin on AgRP neurons in the arcuate nucleus of the hypothalamus. *Journal of*
702 *Comparative Neurology*, 526(1), 133–145. <https://doi.org/10.1002/cne.24327>

- 703 Katz, L. C., & Shatz, C. J. (1996). Synaptic Activity and the Construction of Cortical Circuits.
704 *Science*, 274(5290), 1133–1138. <https://doi.org/10.1126/science.274.5290.1133>
- 705 Kim, J. D., Copperi, F., & Diano, S. (2024). Microglia in Central Control of Metabolism.
706 *Physiology*, 39(1), 5–17. <https://doi.org/10.1152/physiol.00021.2023>
- 707 Kim, J.-S., Kolesnikov, M., Peled-Hajaj, S., Scheyltjens, I., Xia, Y., Trzebanski, S., Haimon, Z.,
708 Shemer, A., Lubart, A., Hove, H. V., Chappell-Maor, L., Boura-Halfon, S., Movahedi, K.,
709 Blinder, P., & Jung, S. (2021). A Binary Cre Transgenic Approach Dissects Microglia and
710 CNS Border-Associated Macrophages. *Immunity*, 54(1), 176-190.e7.
711 <https://doi.org/10.1016/j.immuni.2020.11.007>
- 712 Krashes, M. J., Koda, S., Ye, C., Rogan, S. C., Adams, A. C., Cusher, D. S., ... & Lowell, B. B.
713 (2011). Rapid, reversible activation of AgRP neurons drives feeding behavior in mice. *The*
714 *Journal of clinical investigation*, 121(4), 1424-1428. [https:// www.jci.org/articles/view/46229](https://www.jci.org/articles/view/46229)
- 715 Leyrolle, Q., Layé, S., & Nadjar, A. (2019). Direct and indirect effects of lipids on microglia
716 function. *Neuroscience Letters*, 708, 134348. <https://doi.org/10.1016/j.neulet.2019.134348>
- 717 Li, Q., & Barres, B. A. (2018). Microglia and macrophages in brain homeostasis and disease.
718 *Nature Reviews Immunology*, 18(4), 225–242. <https://doi.org/10.1038/nri.2017.125>
- 719 Li, Q., Cheng, Z., Zhou, L., Darmanis, S., Neff, N. F., Okamoto, J., Gulati, G., Bennett, M. L.,
720 Sun, L. O., Clarke, L. E., Marschallinger, J., Yu, G., Quake, S. R., Wyss-Coray, T., &
721 Barres, B. A. (2019). Developmental Heterogeneity of Microglia and Brain Myeloid Cells
722 Revealed by Deep Single-Cell RNA Sequencing. *Neuron*, 101(2), 207-223.e10.
723 <https://doi.org/10.1016/j.neuron.2018.12.006>
- 724 Li, Y., Du, X., Liu, C., Wen, Z., & Du, J. (2012). Reciprocal Regulation between Resting
725 Microglial Dynamics and Neuronal Activity In Vivo. *Developmental Cell*, 23(6), 1189–1202.
726 <https://doi.org/10.1016/j.devcel.2012.10.027>
- 727 Lippert, R. N., & Brüning, J. C. (2022). Maternal Metabolic Programming of the Developing
728 Central Nervous System: Unified Pathways to Metabolic and Psychiatric Disorders.
729 *Biological Psychiatry*, 91(10), 898–906. <https://doi.org/10.1016/j.biopsych.2021.06.002>
- 730 Masuda, T., Sankowski, R., Staszewski, O., & Prinz, M. (2020). Microglia Heterogeneity in the
731 Single-Cell Era. *Cell Reports*, 30(5), 1271–1281.
732 <https://doi.org/10.1016/j.celrep.2020.01.010>
- 733 Masuyama, H., & Hiramatsu, Y. (2014). Additive Effects of Maternal High Fat Diet during
734 Lactation on Mouse Offspring. *PLoS ONE*, 9(3), e92805.
735 <https://doi.org/10.1371/journal.pone.0092805>
- 736 Miyamoto, A., Wake, H., Ishikawa, A. W., Eto, K., Shibata, K., Murakoshi, H., Koizumi, S.,
737 Moorhouse, A. J., Yoshimura, Y., & Nabekura, J. (2016). Microglia contact induces synapse

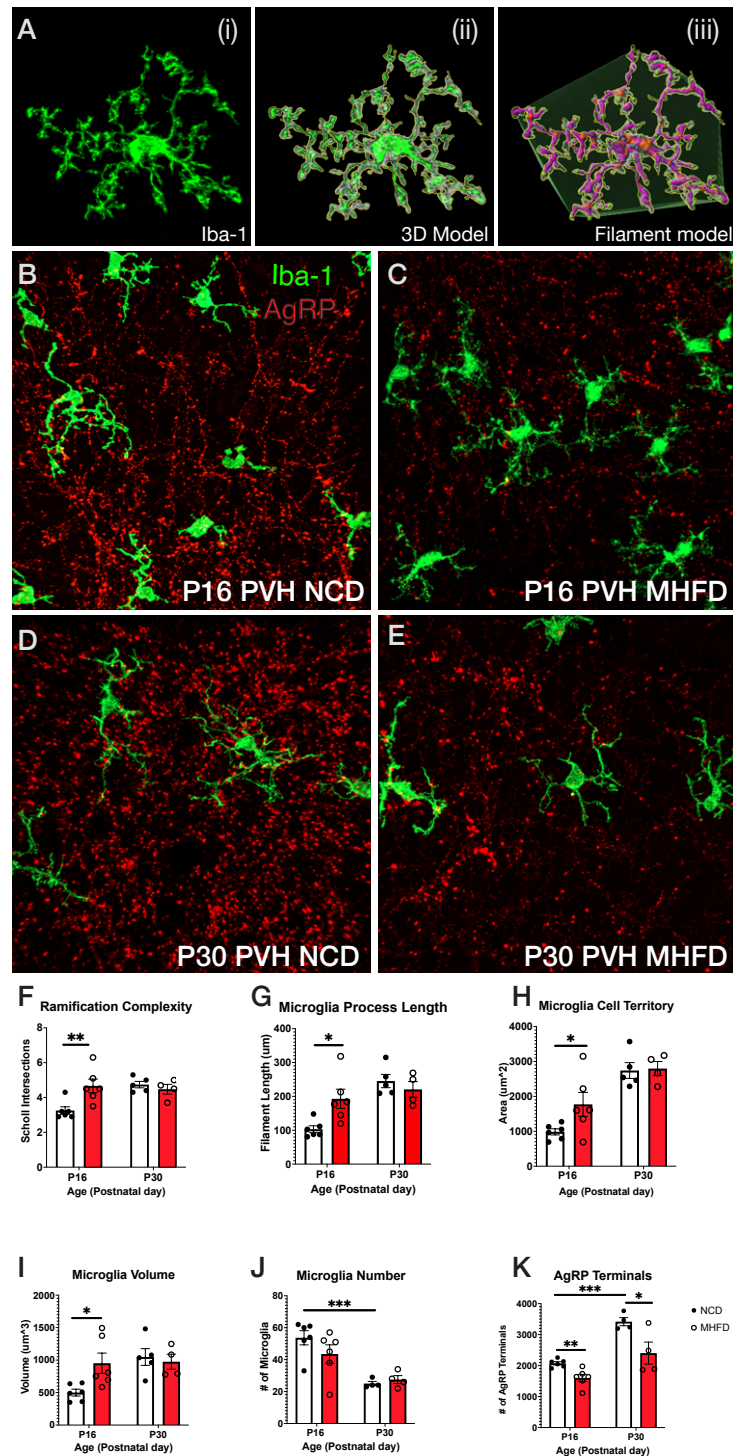
- 738 formation in developing somatosensory cortex. *Nature Communications*, 7(1), 12540.
739 <https://doi.org/10.1038/ncomms12540>
- 740 Morari, J., Anhe, G. F., Nascimento, L. F., Moura, R. F. de, Razolli, D., Solon, C., Guadagnini,
741 D., Souza, G., Mattos, A. H., Tobar, N., Ramos, C. D., Pascoal, V. D., Saad, M. J., Lopes-
742 Cendes, I., Moraes, J. C., & Velloso, L. A. (2014). Fractalkine (CX3CL1) is involved in the
743 early activation of hypothalamic inflammation in experimental obesity. *Diabetes*, 63(11),
744 3770–3784. <https://doi.org/10.2337/db13-1495>
- 745 Nadjar, A., Leyrolle, Q., Joffre, C., & Laye, S. (2017). Bioactive lipids as new class of microglial
746 modulators: When nutrition meets neuroimmunology. *Progress in Neuro-*
747 *Psychopharmacology and Biological Psychiatry*, 79(Pt A), 19–26.
748 <https://doi.org/10.1016/j.pnpbp.2016.07.004>
- 749 Nakajima, K., & Kohsaka, S. (2001). Microglia: Activation and Their Significance in the Central
750 Nervous System. *The Journal of Biochemistry*, 130(2), 169–175.
751 <https://doi.org/10.1093/oxfordjournals.jbchem.a002969>
- 752 Ngozi, Z., & Bolton, J. L. (2022). Microglia Don't Treat All Neurons the Same: The Importance
753 of Neuronal Subtype in Microglia-Neuron Interactions in the Developing Hypothalamus.
754 *Frontiers in Cellular Neuroscience*, 16, 867217. <https://doi.org/10.3389/fncel.2022.867217>
- 755 Ohsawa, K., Irino, Y., Sanagi, T., Nakamura, Y., Suzuki, E., Inoue, K., & Kohsaka, S. (2010).
756 P2Y12 receptor-mediated integrin- β 1 activation regulates microglial process extension
757 induced by ATP. *Glia*, 58(7), 790–801. <https://doi.org/10.1002/glia.20963>
- 758 Paolicelli, R. C., Bolasco, G., Pagani, F., Maggi, L., Scianni, M., Panzanelli, P., Giustetto, M.,
759 Ferreira, T. A., Guiducci, E., Dumas, L., Ragozzino, D., & Gross, C. T. (2011). Synaptic
760 Pruning by Microglia Is Necessary for Normal Brain Development. *Science*, 333(6048),
761 1456–1458. <https://doi.org/10.1126/science.1202529>
- 762 Parkhurst, C. N., Yang, G., Nanan, I., Savas, J. N., Yates, J. R., Lafaille, J. J., Hempstead, B.
763 L., Littman, D. R., & Gan, W.-B. (2013). Microglia Promote Learning-Dependent Synapse
764 Formation through Brain-Derived Neurotrophic Factor. *Cell*, 155(7), 1596–1609.
765 <https://doi.org/10.1016/j.cell.2013.11.030>
- 766 Plagemann, A., Heidrich, I., Götz, F., Rohde, W., & Dörner, G. (1992). Obesity and Enhanced
767 Diabetes and Cardiovascular Risk in Adult Rats due to Early Postnatal Overfeeding.
768 *Experimental and Clinical Endocrinology*, 99(03), 154–158. <https://doi.org/10.1055/s-0029-1211159>
769
- 770 Riquier, A. J., & Sollars, S. I. (2020). Astrocytic response to neural injury is larger during
771 development than in adulthood and is not predicated upon the presence of microglia. *Brain*,
772 *Behavior, & Immunity - Health*, 1, 100010. <https://doi.org/10.1016/j.bbih.2019.100010>

- 773 Rosin, J. M., & Kurrasch, D. M. (2019). Emerging roles for hypothalamic microglia as
774 regulators of physiological homeostasis. *Frontiers in Neuroendocrinology*, 100748.
775 <https://doi.org/10.1016/j.yfrne.2019.100748>
- 776 Samuelsson, A.-M., Matthews, P. A., Argenton, M., Christie, M. R., McConnell, J. M., Jansen,
777 E. H. J. M., Piersma, A. H., Ozanne, S. E., Twinn, D. F., Rémacle, C., Rowlerson, A.,
778 Poston, L., & Taylor, P. D. (2008). Diet-Induced Obesity in Female Mice Leads to Offspring
779 Hyperphagia, Adiposity, Hypertension, and Insulin Resistance: A Novel Murine Model of
780 Developmental Programming. *Hypertension*, 51(2), 383–392.
781 <https://doi.org/10.1161/hypertensionaha.107.101477>
- 782 Sanes, J. R., & Lichtman, J. W. (1999). DEVELOPMENT OF THE VERTEBRATE
783 NEUROMUSCULAR JUNCTION. *Annual Review of Neuroscience*, 22(1), 389–442.
784 <https://doi.org/10.1146/annurev.neuro.22.1.389>
- 785 Schafer, D. P., Lehrman, E. K., Kautzman, A. G., Koyama, R., Mardinly, A. R., Yamasaki, R.,
786 Ransohoff, R. M., Greenberg, M. E., Barres, B. A., & Stevens, B. (2012). Microglia Sculpt
787 Postnatal Neural Circuits in an Activity and Complement-Dependent Manner. *Neuron*, 74(4),
788 691–705. <https://doi.org/10.1016/j.neuron.2012.03.026>
- 789 Schafer, D. P., Lehrman, E. K., & Stevens, B. (2013). The “quad-partite” synapse: Microglia-
790 synapse interactions in the developing and mature CNS. *Glia*, 61(1), 24–36.
791 <https://doi.org/10.1002/glia.22389>
- 792 Simerly, R. B. (2008). Hypothalamic substrates of metabolic imprinting. *Physiology & Behavior*,
793 94(1), 79–89. <https://doi.org/10.1016/j.physbeh.2007.11.023>
- 794 Skowronski, A. A., Leibel, R. L., & LeDuc, C. A. (2023). Neurodevelopmental Programming of
795 Adiposity: Contributions to Obesity Risk. *Endocrine Reviews*, 45(2), 253–280.
796 <https://doi.org/10.1210/endrev/bnad031>
- 797 Spencer, S. J., Basri, B., Sominsky, L., Soch, A., Ayala, M. T., Reineck, P., Gibson, B. C., &
798 Barrientos, R. M. (2019). High-fat diet worsens the impact of aging on microglial function
799 and morphology in a region-specific manner. *Neurobiology of Aging*, 74, 121–134.
800 <https://doi.org/10.1016/j.neurobiolaging.2018.10.018>
- 801 Stephan, A. H., Barres, B. A., & Stevens, B. (2012). The Complement System: An Unexpected
802 Role in Synaptic Pruning During Development and Disease. *Neuroscience*, 35(1), 369–389.
803 <https://doi.org/10.1146/annurev-neuro-061010-113810>
- 804 Stettler, N., Stallings, V. A., Troxel, A. B., Zhao, J., Schinnar, R., Nelson, S. E., Ziegler, E. E.,
805 & Strom, B. L. (2005). Weight gain in the first week of life and overweight in adulthood: a
806 cohort study of European American subjects fed infant formula. *Circulation*, 111(15), 1897–
807 1903. <https://doi.org/10.1161/01.cir.0000161797.67671.a7>

- 808 Stevens, B., Allen, N. J., Vazquez, L. E., Howell, G. R., Christopherson, K. S., Nouri, N.,
809 Micheva, K. D., Mehalow, A. K., Huberman, A. D., Stafford, B., Sher, A., Litke, A. M.,
810 Lambris, J. D., Smith, S. J., John, S. W. M., & Barres, B. A. (2007). The Classical
811 Complement Cascade Mediates CNS Synapse Elimination. *Cell*, 131(6), 1164–1178.
812 <https://doi.org/10.1016/j.cell.2007.10.036>
- 813 Stowell, R. D., Wong, E. L., Batchelor, H. N., Mendes, M. S., Lamantia, C. E., Whitelaw, B. S.,
814 & Majewska, A. K. (2018). Cerebellar microglia are dynamically unique and survey Purkinje
815 neurons in vivo. *Developmental Neurobiology*, 78(6), 627–644.
816 <https://doi.org/10.1002/dneu.22572>
- 817 Sun, J., Wang, X., Sun, R., Xiao, X., Wang, Y., Peng, Y., & Gao, Y. (2023). Microglia shape
818 AgRP neuron postnatal development via regulating perineuronal net plasticity. *Molecular*
819 *Psychiatry*, 1–11. <https://doi.org/10.1038/s41380-023-02326-2>
- 820 Sutton Hickey, A. K., Duane, S. C., Mickelsen, L. E., Karolczak, E. O., Shamma, A. M.,
821 Skillings, A., ... & Krashes, M. J. (2023). AgRP neurons coordinate the mitigation of
822 activity-based anorexia. *Molecular psychiatry*, 28(4), 1622-1635.
823 <https://doi.org/10.1038/s41380-022-01932-w>
- 824 Tamashiro, K. L. K., & Moran, T. H. (2010). Perinatal environment and its influences on
825 metabolic programming of offspring. *Physiology & Behavior*, 100(5), 560–566.
826 <https://doi.org/10.1016/j.physbeh.2010.04.008>
- 827 Thaler, J. P., Yi, C.-X., Schur, E. A., Guyenet, S. J., Hwang, B. H., Dietrich, M. O., Zhao, X.,
828 Sarruf, D. A., Izgur, V., Maravilla, K. R., Nguyen, H. T., Fischer, J. D., Matsen, M. E., Wisse,
829 B. E., Morton, G. J., Horvath, T. L., Baskin, D. G., Tschöp, M. H., & Schwartz, M. W. (2012).
830 Obesity is associated with hypothalamic injury in rodents and humans. *Journal of Clinical*
831 *Investigation*, 122(1), 153–162. <https://doi.org/10.1172/jci59660>
- 832 Town, T., Nikolic, V., & Tan, J. (2005). The microglial “activation” continuum: from innate to
833 adaptive responses. *Journal of Neuroinflammation*, 2(1), 24. <https://doi.org/10.1186/1742-2094-2-24>
- 835 Tremblay, M.-È., Lowery, R. L., & Majewska, A. K. (2010). Microglial Interactions with
836 Synapses Are Modulated by Visual Experience. *PLoS Biology*, 8(11), e1000527.
837 <https://doi.org/10.1371/journal.pbio.1000527>
- 838 Tremblay, M.-È., Stevens, B., Sierra, A., Wake, H., Bessis, A., & Nimmerjahn, A. (2011). The
839 Role of Microglia in the Healthy Brain. *The Journal of Neuroscience*, 31(45), 16064–16069.
840 <https://doi.org/10.1523/jneurosci.4158-11.2011>
- 841 Valdearcos, M., Douglass, J. D., Robblee, M. M., Dorfman, M. D., Stifler, D. R., Bennett, M. L.,
842 Gerritse, I., Fasnacht, R., Barres, B. A., Thaler, J. P., & Koliwad, S. K. (2017). Microglial
843 Inflammatory Signaling Orchestrates the Hypothalamic Immune Response to Dietary

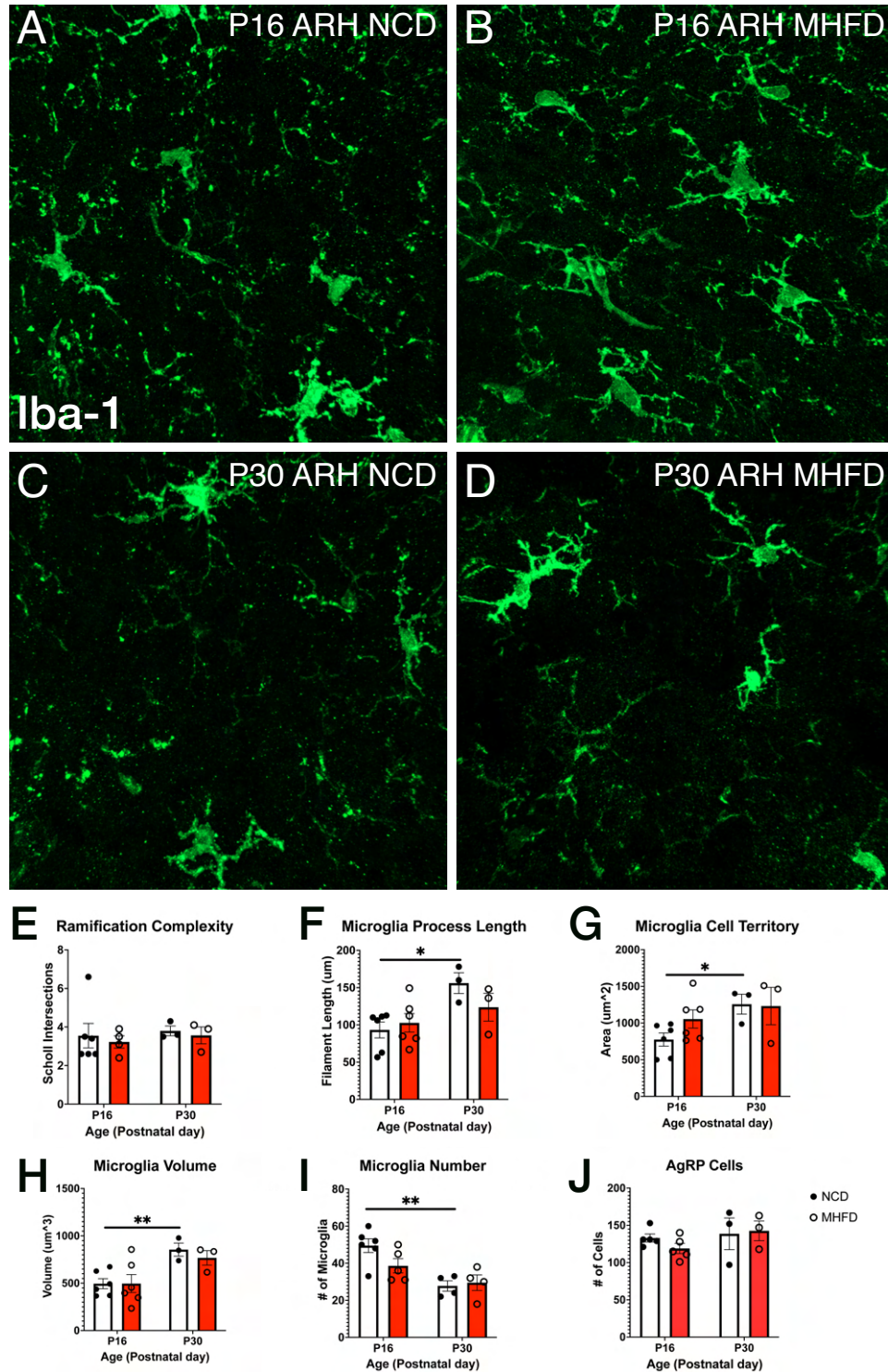
- 844 Excess and Mediates Obesity Susceptibility. *Cell Metabolism*, 26(1), 185-197.e3.
845 <https://doi.org/10.1016/j.cmet.2017.05.015>
- 846 Valdearcos, M., Robblee, M. M., Benjamin, D. I., Nomura, D. K., Xu, A. W., & Koliwad, S. K.
847 (2014). Microglia Dictate the Impact of Saturated Fat Consumption on Hypothalamic
848 Inflammation and Neuronal Function. *Cell Reports*, 9(6), 2124–2138.
849 <https://doi.org/10.1016/j.celrep.2014.11.018>
- 850 Vogt, M. C., Paeger, L., Hess, S., Steculorum, S. M., Awazawa, M., Hampel, B., Neupert, S.,
851 Nicholls, H. T., Mauer, J., Hausen, A. C., Predel, R., Kloppenburg, P., Horvath, T. L., &
852 Brüning, J. C. (2014). Neonatal Insulin Action Impairs Hypothalamic Neurocircuit Formation
853 in Response to Maternal High-Fat Feeding. *Cell*, 156(3), 495–509.
854 <https://doi.org/10.1016/j.cell.2014.01.008>
- 855 Wake, H., Moorhouse, A. J., Jinno, S., Kohsaka, S., & Nabekura, J. (2009). Resting Microglia
856 Directly Monitor the Functional State of Synapses In Vivo and Determine the Fate of
857 Ischemic Terminals. *The Journal of Neuroscience*, 29(13), 3974–3980.
858 <https://doi.org/10.1523/jneurosci.4363-08.2009>
- 859 Wang, C., Yue, H., Hu, Z., Shen, Y., Ma, J., Li, J., Wang, X.-D., Wang, L., Sun, B., Shi, P.,
860 Wang, L., & Gu, Y. (2020). Microglia mediate forgetting via complement-dependent synaptic
861 elimination. *Science*, 367(6478), 688–694. <https://doi.org/10.1126/science.aaz2288>
- 862 Wong, A. M., Patel, N. V., Patel, N. K., Wei, M., Morgan, T. E., Beer, M. C. de, Villiers, W. J. S.
863 de, & Finch, C. E. (2005). Macrosialin increases during normal brain aging are attenuated
864 by caloric restriction. *Neuroscience Letters*, 390(2), 76–80.
865 <https://doi.org/10.1016/j.neulet.2005.07.058>
- 866 Young, A. M., Kumasaka, N., Calvert, F., Hammond, T. R., Knights, A., Panousis, N., Park, J.
867 S., Schwartzenuber, J., Liu, J., Kundu, K., Segel, M., Murphy, N. A., McMurrin, C. E.,
868 Bulstrode, H., Correia, J., Budohoski, K. P., Joannides, A., Guilfoyle, M. R., Trivedi, R., ...
869 Gaffney, D. J. (2021). A map of transcriptional heterogeneity and regulatory variation in
870 human microglia. *Nature Genetics*, 53(6), 861–868. [https://doi.org/10.1038/s41588-021-](https://doi.org/10.1038/s41588-021-00875-2)
871 [00875-2](https://doi.org/10.1038/s41588-021-00875-2)
- 872 Zagmutt, S., Mera, P., Soler-Vázquez, M. C., Herrero, L., & Serra, D. (2018). Targeting AgRP
873 neurons to maintain energy balance: Lessons from animal models. *Biochemical*
874 *Pharmacology*, 155, 224–232. <https://doi.org/10.1016/j.bcp.2018.07.008>
- 875 Zeltser, L. M. (2018). Feeding circuit development and early-life influences on future feeding
876 behaviour. *Nature Reviews Neuroscience*, 19(5), 302–316.
877 <https://doi.org/10.1038/nrn.2018.23>
- 878
- 879

880
881 **Figures**



882
883
884 **Figure 1. MHFD: Microglial morphology in the PVH.** (A) Image analysis pipeline. Maximum projection
885 of an Iba1 stained microglial cell in the PVH (Ai). Confocal images through labeled cells were used to

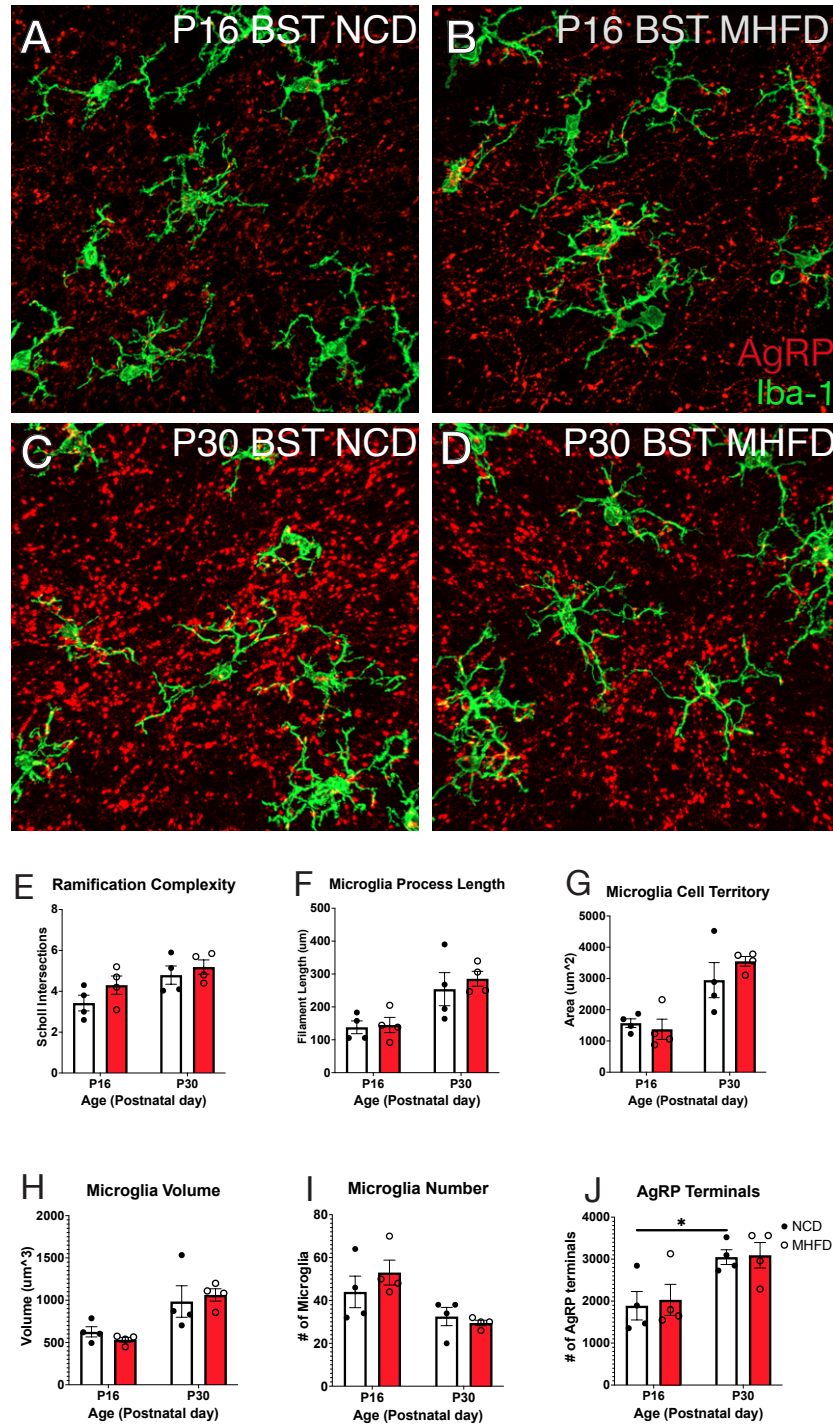
886 generate 3D reconstructions (Aii). Each 3D rendering was then used to create a skeletonized model by
887 using the Filaments tool in Imaris. Polyhedrons were generated around each cell using the Convex Hull
888 function of Imaris to estimate the total tissue “territory” occupied by the microglial cell (Aiii). (B-E)
889 Maximum projection images of microglial cells (green) and labeled AgRP terminals (red) in the PVH of
890 mice at P16 (B,C) or P30 (D,E) that were either exposed to MHFD (C, E) or NCD (B, D). (F-J) Graphical
891 comparisons between groups to show that MHFD increased microglial ramification complexity (F),
892 microglial cell territory (G), cell volume (H) and process length (I) and AgRP terminals (K). The density of
893 microglia in the PVH decreased between P16 and P30, irrespective of diet (J). Bars represent the mean \pm
894 SEM and each point represents one animal. *P<.05, **P<.005. Abbreviations: MHFD, maternal high fat
895 diet during lactation; NCD, Normal Chow Diet; PVH, paraventricular nucleus of the hypothalamus.
896



897
898
899
900
901
902
903

Figure 2. MHFD: Microglial morphology in the ARH. Maximum projection images of microglial cells (green) in the ARH of mice at P16 (A, B) or P30 (C, D) that were either exposed to MHFD (B, D) or NCD (A, C). Graphical comparisons between groups to show that microglial ramification complexity (E) remained the same, regardless of age or diet. Microglial cell territory (F), cell volume (G) and process length (H) increased between P16 and P30, but were not changed as a result of diet. The density of

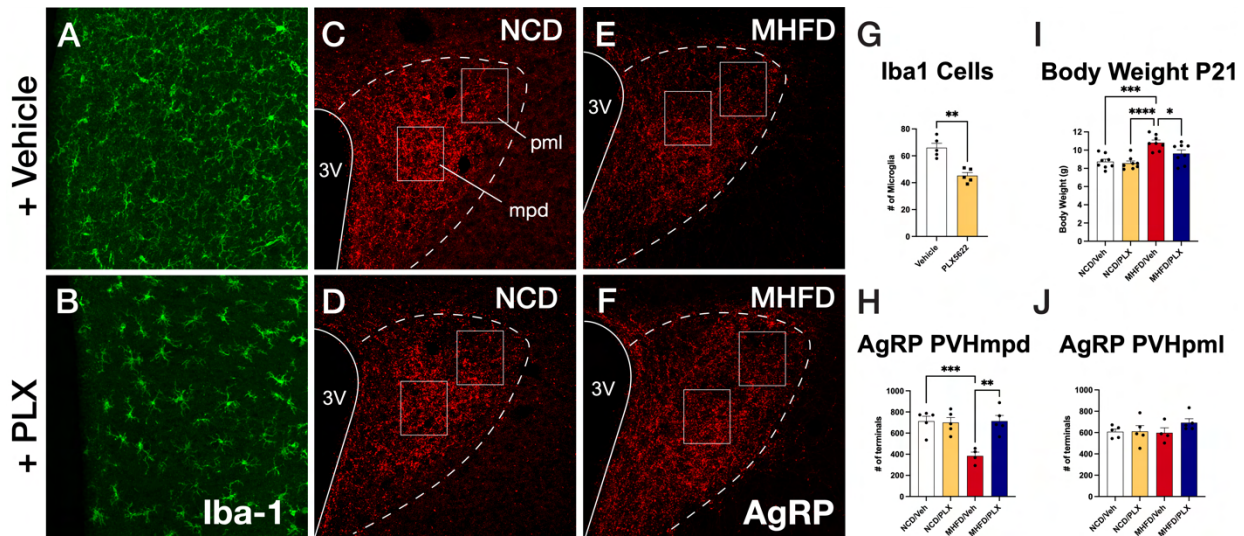
904 microglia in the ARH decreased between P16 and P30, irrespective of diet (I). There were no changes in
905 numbers of AgRP neurons (J). Bars represent the mean \pm SEM and each point represents one animal.
906 * $P < .05$, ** $P < .005$. Abbreviations: ARH, arcuate nucleus of the hypothalamus; MHFD, maternal high fat
907 diet during lactation; NCD, Normal Chow Diet.
908



909 **Figure 3. MHFD: Microglial morphology in the BST.** Maximum projection images of microglial cells
910 (green) and labeled AgRP terminals (red) in the BST of mice at P16 (A, B) or P30 (C, D) that were either
911 exposed to MHFD (B, D) or NCD (A, C). Graphical comparisons between groups to show that microglial
912

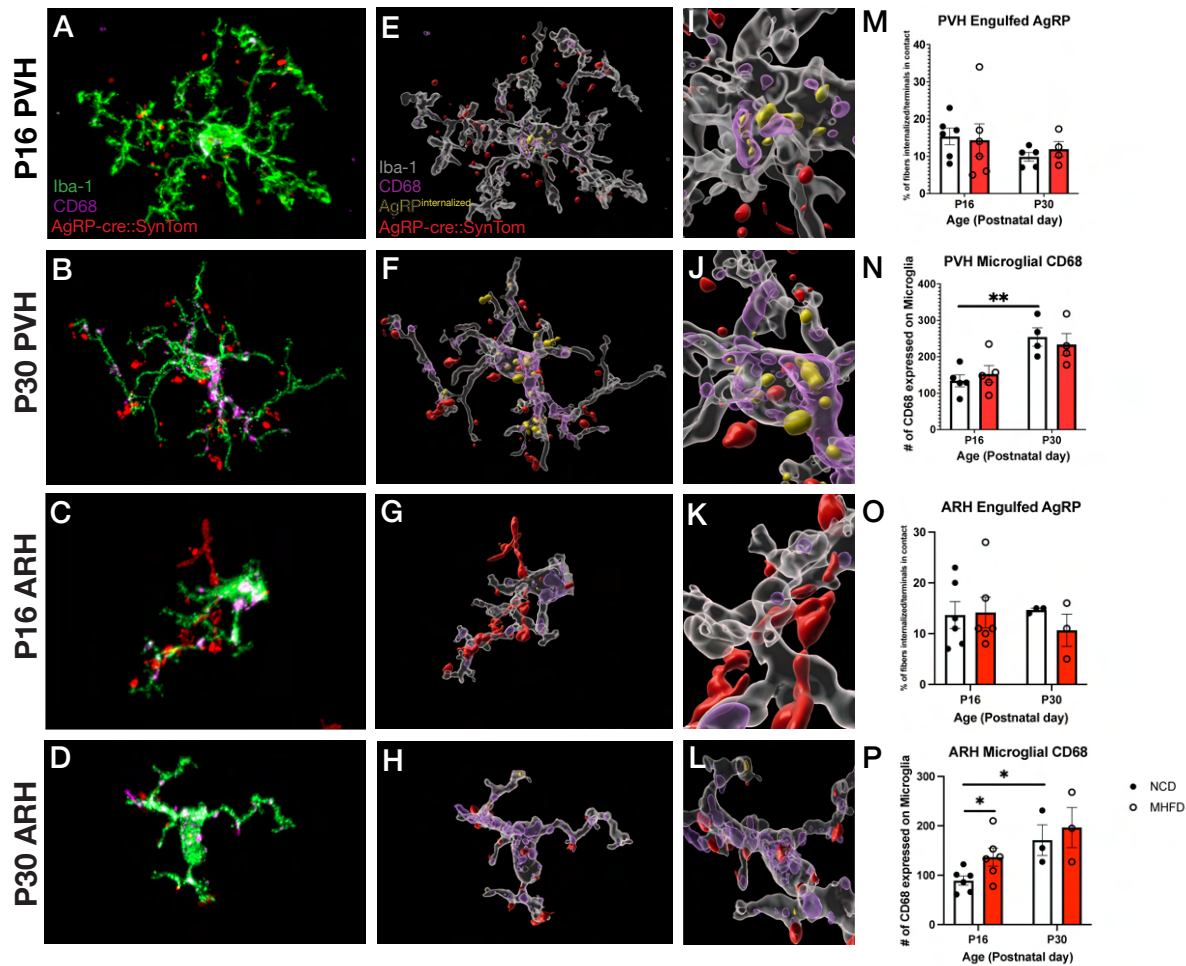
913 ramification complexity (E) remained the same, regardless of age or diet. Microglial cell territory (F), cell
 914 volume (G) and process length (H) did not significantly change between P16 and P30 and were not
 915 changed as a result of diet. The density of microglia in the BST decreased between P16 and P30,
 916 irrespective of diet (I). The density of AgRP terminals increased between P16 and P30, but there was no
 917 effect of maternal diet (J). Bars represent the mean \pm SEM and each point represents one animal.
 918 * $P < .05$. Abbreviations: BST, bed nucleus of the stria terminalis; MHFD, maternal high fat diet during
 919 lactation; NCD, Normal Chow Diet.

920
 921
 922



923
 924
 925 **Figure 4. Microglial depletion during lactation period.** Images of microglial cells (green) to assess
 926 microglia number (A,B). Maximum projection images of labeled AgRP terminals (red) to assess AgRP
 927 terminal density in distinct compartments of the PVH at P55 long after the period of daily injections (C-F).
 928 Graphical comparison between groups to show that daily postnatal PLX5622 injections caused a 33%
 929 decrease in microglia in the PVH (G). Maximum projections of confocal images to illustrate the density of
 930 AgRP labeling in the PVH of NCD offspring (C,D) and MHFD offspring (E,F). (G-J) Graphical comparison
 931 to illustrate the effects of postnatal PLX5622 treatments on microglia in the PVH (G), body weight (I) and
 932 the density of AgRP terminals in the PVHmpd (H) and PVHpml (J). Bars represent the mean \pm SEM and
 933 each point represents one animal. * $P < .05$, ** $P < .005$, *** $P < .0005$. Abbreviations: AgRP, agouti-related
 934 peptide; CSF1R, Colony-Stimulating Factor 1 Receptor; MHFD, maternal high fat diet during lactation;
 935 MPD, medial parvocellular compartment of the PVH; PML, posterior magnocellular compartment of the
 936 PVH; PVH, paraventricular nucleus of the hypothalamus.
 937

938



939

940

941 **Figure 5. Microglial interaction with AgRP axon terminals in the PVH and ARH.** (A-D) Maximum

942 projection images of microglial cells (green) labeled AgRP terminals (red), and CD68 (lysosomal

943 associated membrane protein and phagocytic capacity marker, pink). (E-H) Digital 3D reconstructions

944 shown in (A-D) after application of a digital zoom to more clearly illustrate engulfment of labeled AgRP

945 terminals by microglia (I-L). (M-P) Graphical comparisons between groups to illustrate the effects of age

946 and MHFD exposure on CD68 expression and AgRP terminal engulfment. Bars represent the mean \pm

947 SEM and each point represents one animal. * $P < .05$, ** $P < .005$. Abbreviations: AgRP, agouti-related

948 peptide; ARH, arcuate nucleus or the hypothalamus; CD68, Cluster of Differentiation 68; MHFD, maternal

949 high fat diet during lactation; PVH, paraventricular nucleus of the hypothalamus.